Spatial Association Analysis Between Hydrocarbon Fields and Sedimentary Résidual Magnetic Anomalies: A Case Study from the Algerian Triassic Province

K. Allek, A. Bouguern
Laboratory of Earth Physics, University of Boumerdes, Algeria
D. Boubaya
University of Tebessa, Algeria
M. Hamoudi
USTHB University, Algiers, Algeria

ABSTRACT The presence of Sedimentary Residual Magnetic (SRM) anomalies over hydrocarbon accumulations and their contribution to exploration remain somewhat controversial despite encouraging results and an improved understanding of genetic links between hydrocarbon seepage-induced alterations and near-surface magnetic minerals. These uncertainties still exist because shallow-sourced SRM anomalies are not associated exclusively with hydrocarbon. The cause of these anomalies may well be microseepage related, *but* could also *result* from others sources such as cultural features or detrital magnetite. To deal with this particular purpose, we explore the spatial association between known hydrocarbon fields within the Algerian Triassic province basin and SRM anomalies using GIS-based weights of evidence statistical approach. The results indicate that the known hydrocarbon fields are strongly associated with particular classes of anomalies. These results are significantly useful for further exploration in the case of the study region, and can also be extended to regions with similar characteristics.

1 INTRODUCTION

Airborne magnetic surveying has been used in oil exploration for many decades. It traditionally applied to quickly and economically screen large areas for mapping depths to basement and bedrock structures that control emplacement of hydrocarbon in overlying sedimentary basins. Recent years have seen a surge in interest for the application of magnetic data to the detection of intra-sedimentary shallow-sourced anomalies associated with hydrocarbon microseepages. It has been well documented that most oil and gas accumulations leak hydrocarbons, creating alteration features close to the surface that can be identified using geochemical methods as well as any of geophysical techniques such as gamma-ray spectrometry, induced polarization and magnetic (Saunders et al., 1993; Foote, 1996; Schumacher, 2000; Peres-Peres 2011; Curto et al., 2012; Flekkoy et al., 2013).

The first time that has been shown the presence of magnetic anomalies in levels near surface, associated with the presence of underlying hydrocarbon deposits was in late seventies. It was made independently by Donovan et al. (1979) and by Berezkin et al. (1978). Advances made in processing aeromagnetic data and an improved understanding of seep mechanisms and alteration processes that could result in formation of authigenic (formed in place) magnetic minerals has promoted the magnetic method from a reconnaissance tool to a valuable exploration technique for detecting hydrocarbon by mapping short wavelength magnetic anomalies assumed to be in relationship with hydrocarbon seep-induced near-surface magnetic minerals, either in onshore or offshore basins (Foote, 1996; Burazer et al., 2001; Stone et al., 2004; Curto et al., 2012; Schumacher and Foote, 2014; Menshov et al., 2014). This seep-induced magnetic minerals has led to some development of analytical methods that allow subtle anomaly identification. Foote (1996) developed a method referred to as "Magnetic Bright Spots (MBS)" - which provide valuable clues to an underlying oil or gas accumulation. Studies from onshore and offshore examples (Schumacher and Foote, 2006; 2014) reveal stunning results. The exploration leads and prospects associated with a MBS anomaly are 4 to 6 times more likely to result in a commercial oil or gas discovery than a similar prospect without such an anomaly. Stone et al. (2004) described a simple micromagnetic aureole search methodology which is intended to the recognition of annular/aureole-shaped anomalies. The test study from a high-resolution aeromagnetic survey performed over Muglad Basin of southern Sudan has successfully revealed an annular anomaly correlating directly with the Jarayan oil field.

Despite the good consistency of results obtained from published studies, this method did not penetrate into subconsciousness of practicing geophysicists from industry. If data processing techniques can often remove the influence of deep magnetic basement rocks, this is not always the case when it comes to discriminate between the effects of

shorter wavelengths anomalies which can result both from authigenic ferromagnetic minerals than possible syngenetic magnetic sources. Gay and Hawley (1991) and Gay (1992) remained skeptical about the origin of near-surface intra-sedimentary magnetic anomalies supposedly caused by hydrocarbon microssepages. They cite examples of many false anomalies caused by detrital magnetite, tuffs, "black sands" in stream channels and cultural contamination from surface and near-surface iron. It is this skepticism that appears to deter many petroleum geophysicists.

Because of this controversy about the presence, origin, and exploration significance of magnetic mineralization associated with hydrocarbon accumulations, we decide to carry out a more analytical and more objective methodology, using GIS-based Weights of Evidence (WofE) approach to verify the genetic links between SRM anomalies and hydrocarbon seepage environments. This method has been extensively applied for mineral potential mapping; however, the present study represents its first application to hydrocarbons exploration. The Oued Mya Basin which contains numerous oil and gas producing fields as well as the giant gas-deposit of Hassi R'mel provides an ideal case study.

Our aim was to investigate the spatial association between SRM anomalies and the known hydrocarbon fields within the study area to answer the question whether the spatial distribution of these magnetic anomalies is controlled by the underlying oil/gas fields. First, we use the WofE technique to establish a quantitative characterization of the spatial relationship. Next, we reveal the characteristics (wavelengths and amplitudes) of the type of anomalies assumed to be induced by hydrocarbon microseepages. Finally, we show evidence of the convenience of large-scale aeromagnetic data for such tasks when acquired at relatively low altitude and at suitable accuracy.

2 HYDROCARBON SEEPS

It has long been recognized that most oil and gas accumulations leak hydrocarbons due to high pressures at depth. This leakage occurs vertically or near-vertically from the reservoir to the surface through fractures in rocks and planes of weakness between geological layers or along fault discontinuities (Schumacher, 2010, Salati, 2014). Except some macro-seeps encountered sometimes in certain regions, that manifest themselves as the visible presence of oil and gas seeping to the surface, most of hydrocarbon seeps have no visible and direct evidences of their presence (microseeps), but cause several chemical reactions and microbial oxidation in the rocks and soils and also cause changes in Eh and pH. Such changes in the near-surface soils destabilize many compounds, increase the solubility of the elements and induce mineralogical alterations such as red beds bleaching, clays formation, and creation of secondary carbonates, sulfides, and magnetic minerals (Schumacher, 1996; 2014; Srinivasan et al. 2014; Salati, 2014).

Eventov (1997) have reviewed some of the most documented theories concerning the formation of the diagenetic magnetite, caused by hydrocarbon seepages. According to these theories, the hydrocarbon-induced reducing environment can lead to the precipitation of a variety of magnetic iron oxides and sulfides, including magnetite (Fe_3O_4), maghemite (γ-Fe_2O_3), pyrrhotite (Fe_7S_8), and greigite (Fe_3S_4). Schumacher (1996) provided a model for hydrocarbon-induced magnetic minerals. In accordance with this model, upward-migrating light hydrocarbons reach near-surface oxidizing conditions, aerobic hydrocarbon-oxidizing bacteria consume methane (and other light hydrocarbons) and decrease oxygen in pore waters. With development of anaerobic conditions, the activity of sulfate-reducing bacteria results in

sulfate ion reduction and oxidation of organic carbon to produce bicarbonate ion and reduced sulfur species which in turn combine with available iron to form iron sulfides and oxides. For their part, Machel and Burton (1991) suggested that magnetic minerals could be either produced or destroyed under the influence of hydrocarbons seeps. On the basis of extensive investigations conducted in major oil fields of several basins in China, the results of mineralogical analysis reveal that the enhanced magnetic susceptibility relating to the hydrocarbon microssepages are caused by secondary magnetite and the subsequent low-temperature oxidation products (maghemite) (Liu et al., 2004).

Diagenetic magnetic minerals created by hydrocarbon microseepage have been reported to occur over a wide range in *depth*, from surface soils to strata as deep as 1500 m (LeSchack and Van Alstine, 2002). The identification of anomalous magnetic minerals over oil and gas accumulations has been established by magnetic susceptibility measurements and magnetic mineralogy analysis of surface soils, drill cuttings and cores from oil wells. Saunders et al. (1991) documented increases in magnetic susceptibility that were caused by high concentrations of authigenic magnetic minerals (magnetite and probably maghemite) occurring just

below the grass roots. Foote (1996) reported that most magnetically enhanced zones detected in high resolution ground and airborne magnetic surveys over hydrocarbon reservoirs are thought to occur at depths of 60–600 m. Peres-Peres et al. (2011) revealed the presence of authigenic magnetite at a depth of about 600 m by analyzing drill cuttings from Venezuelan and Colombian oil fields.

3 MATERIALS AND METHODS

3.1 Study area

This study was developed in a region within the Triassic province of Algeria, in fact a large basin located on the northern-central part of the Saharan Platform. It lies at the Northern part of the Oued Mya depression, between 0° 40' - 4° 48'E longitudes and 31° 06' - 33° 55'N latitudes. This study region as a whole consists of a number of structural units: Djorfa saddle, Tilrhemt dome, and parts of the Benoud trough and Touggourt saddle (Fig. 1).

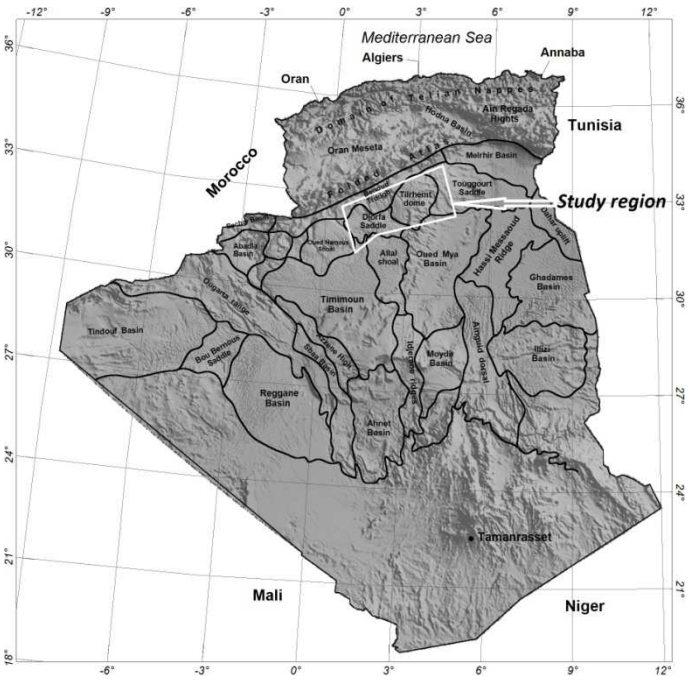

Figure 1. Algerian territory, showing defined structural units and the study area location.

The current structural scheme is the result of several tectonic phases which the most important are the Panafrican, the Hercynian, the Triassic-Jurassic extension, the Austrian, and the major Alpine phase. The Tilrhemt dome is the most important anticline structure in the region with ENE-WSW direction, and probably Hercynian age. According to the geological map, mostly Cretaceous formations outcrop in this area, whereas Neogene-Oligocene and sand dunes dominate in the rest of the region (Fig. 2).

The study area contains the giant Hassi R'mel gas field and numerous oil and gas deposits exploited at the Triassic and Cambrian-Ordovician levels. The Saharan Triassic which is the main petroleum objective, consists of sediments of varied continental environments; namely, fluvial, floodplain, lake, sebkha, and wind (Baouche et al., 2009). The region was first investigated in 1951 which led to the drilling of the first well south of Berriane. The encouraging results led to the discovery of the Hassi R'mel field in 1956, which was put on production in 1961 and proved to be one of the world's largest gas fields. The Field extends 70 km from north to south and 50 km from east to west (Bencherif, 2003). Exploration increased the subsequent decades leading to the discovery of several oil and gas fields in the region.

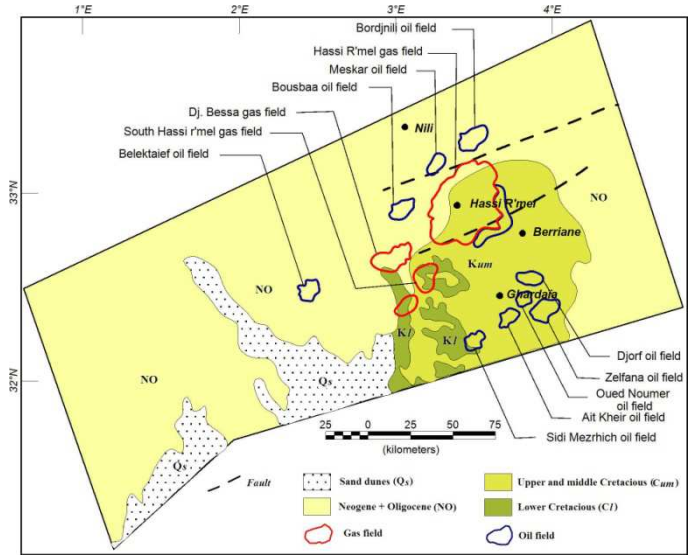

Figure 2. Simplified geological map and oil-gas fields location

3.2 Survey

The regional airborne magnetic survey over the Oued Mya region was part of the nationwide aeromagnetic survey of Algeria. The survey was completed by Aeroservices Limited in 1974 on behalf of the *SONAREM* (*Société Nationale de la Recherche et d'Exploitation Minière*). The aeromagnetic data were acquired with a nominal terrain clearance of 150 meters using a high resolution (0.02 nT) optically pumped cesium vapor magnetometer. Traverse lines were oriented N160° (NNW-SSE), with a spacing of 5 km. Tie-lines (Control-lines) were oriented perpendicular to traverse lines with a spacing of 25 km. Tie-lines were also flown along the survey boundary when not parallel to the traverse line direction. Readings were taken at one-second intervals, yielding at an average aircraft speed of 165 km/h a magnetic measurement about every 46 m along the flight path. The survey

contains 13,980 line-kilometers, and covers surface of 56,900 km². Variations in the magnetic field resulting from different aircraft induced noise were electronically compensated.

In order to ensure the *quality* of measurements, the maximum diurnal change allowed was less than 3 nT for any 3-minute chord (period) of time. Data were re-acquired when this condition is exceeded, with any re-flown line segment crossing a minimum of two control lines. Several data processing procedures: such as tie-line leveling, IGRF calculation and removal, lag effect correction and microlevelling, were carefully achieved to get the most out of the detection of subtle anomalies. Although this survey is very widely spaced, it is acquired at a relatively low height, and there are sufficient reading along each flight line such that micromagnetic anomalies close to flight lines are well identified.

3.3 Enhancement of SRM anomalies

It should be noted that for airborne magnetic data, the flight altitude, sample spacing along flight lines and line spacing play an important role in the detection of high wavenumber weak magnetic anomalies. In Algeria, most available aeromagnetic surveys were accomplished at the reconnaissance scale and, thus far they have been mostly used to define the main basin structural features. On the other hand, They are at an accuracy and at a height that makes them suitable for the detection of subtle anomalies when they are close to a flight line. However, processing the survey as grided data would tend to obscure any isolated narrow anomalies. That's why all filtering computations, performed in this study to isolate subtle anoamlies, were carried out on profile data.

To highlight Sedimentary Residual Magnetic (SRM) anomalies, the most contentious problems are to remove cultural influence and basement magnetic signal. These SRM anomalies are often masked by much stronger magnetic anomalies caused by underlying magnetic formations and/or by cultural features. However, if the basement magnetic sources generally can be distinguished by their large wavelenghts, this is not always the case when one has to do with the cultural sources. Randomly scattered oil well casings, metal storage tanks, pipelines, and other cultural features on or near the ground surface alters magnetic data acquired for hydrocarbon microseepage purposes. These sources create short-wavelength high-amplitude signatures in total field magnetic intensity maps and they can mask the effect of seep-induced anomalies and sometimes even confused with them.

We used the radial power spectra of the anomalous field (Spector and Grant 1970) to help distinguish anomalies caused by near-surface intrasedimentary sources from anomalies caused by cultural sources and those from basement rocks. The diagenetic magnetic signal is generally recognized by its longer “wavelength” (compared to cultural features and background noise). The very long basement effects and very short cultural sources were removed by applying a selective band-pass filter. Afterward, amplitudes of the Analytic Signal of the isolated Sedimentary Residual Magnetic (AS-SRM) anomalies were calculated to deal with distortion and polarity effects of anomalies so that they can be more easier studied and categorized.

4 SPATIAL ANALYSIS APPROACH

4.1 Weights of Evidence method

Weights of evidence (*WofE*) is a Bayesian statistical method for assessing the degree of spatial association and for combining evidence to test a hypothesis. It determines the probability of an event to occur under certain conditions. The method was originally developed for a non-spatial application in medical diagnosis, later it was extensively used for mineral potential mapping in a GIS environment (Bonham-Carter, 1994), and soon after adapted for landslide susceptibility analysis, hazard modeling, fires and so on. The WofE method is applied here to investigate the spatial associations between interpreted Sedimentary Residual Magnetic (SRM) anomalies and mapped hydrocarbon fields within the Oued Mya Basin. The importance of the weights depends on the measured association and permits to provide an insight into the characteristics of the SRM anomalies related to seep-induced magnetic minerals. This method could be used as spatial evidence in hydrocarbon prospectivity mapping.

A detailed explanation of the mathematical formulation of the WofE modeling method is available in Bonham-Carter (1994). The method uses a log-linear of the Bayesian probability model to estimate the importance of evidences by a pair of weights, one (positive weight W^+) for presence of the evidence H, and negative weight (W^-) for absence of the evidence H.

$$W^+ = ln\left(\frac{P(H|A)}{P(H|\bar{A})}\right) \qquad (1)$$

$$W^- = ln\left(\frac{P(\bar{H}|A)}{P(\bar{H}|\bar{A})}\right) \qquad (2)$$

where P() denotes probability, H is the presence of hydrocarbon pattern (it corresponds to area occupied by hydrocarbon field), $\bar{H}$ is the absence of hydrocarbon pattern, A is the presence of points of interest (corresponds to center-points of picked SRM anomalies), $\bar{A}$ is the absence of points occurrence.

The weights (W^+ *and* W^-) provide a measure of spatial association between the training points and the binary theme H. They are calculated for each class of the picked SRM anomalies. The value of the weight W^+ is positive, whereas W^- is negative, indicates that there are more SRM anomalies on binary theme H than would occur due to chance. Conversely W^+ would be negative and W^- positive for the case where fewer points occur than expected. If the picked anomalies A are distributed randomly with respect to the binary theme H, then both of weights will have a value of zero, or very close to zero.

The difference between the weights is known as the contrast, C. Thus:

$$C = W^+ - W^- \qquad (3)$$

The contrast is an overall measure of spatial association between the set of points A and the binary theme H, combining the effects of the two weights. It is the best estimator in a large area and when a large number of points occurrences are considered (Bonham-Carter, 1994). Hence, for a positive correlation, C is positive; C is negative in the case of negative spatial correlation.

The studentized confidence value *s(C)*, defined as the contrast *C* divided by its standard deviation, corresponds approximately to the statistical level of significance defined by standard z-tests, and provides a useful measure of the significance of the contrast (Raines, 1999). The standard deviation of C is calculated as:

$$s(C) = \sqrt{s^2(W^+) + s^2(W^-)} \qquad (4)$$

In the spatial analysis, as applied in this work, a simplified and intuitive approach similar to that suggested by Turner (1997), was adopted. The surface of the study area and the binary pattern H are expressed in number of unit cells, and each training point is assumed to occupy a single unit cell. That way, the weights W^+ and W^- can be calculated by means of map crossing functions as follows:

$$W^+ = ln\left(\frac{\frac{Number\ of\ points\ A\ (picked\ anomalies)\ \boldsymbol{inside}\ the\ pattern\ H}{Total\ number\ of\ \ points\ A}}{\frac{Number\ of\ unit\ cells\ \boldsymbol{inside}\ pattern\ H\ not\ occupied\ by\ points\ A}{Total\ number\ of\ unit\ cells\ of\ the\ study\ area\ not\ occupied\ by\ points\ A}}\right) \qquad (5)$$

$$W^- = ln\left(\frac{\frac{Number\ of\ points\ A\ \boldsymbol{outside}\ the\ pattern\ H}{Total\ number\ of\ points\ A}}{\frac{Number\ of\ unit\ cells\ \boldsymbol{outside}\ pattern\ H\ not\ occupied\ by\ points\ A}{Total\ number\ of\ unit\ cells\ of\ the\ study\ area\ not\ occupied\ by\ points\ A}}\right) \qquad (6)$$

A unit cell of 1 km x 1 km was used. This was chosen for two reasons: the scale of the present aeromagnetic survey, and expected dimensions of SRM anomalies so that each cell can contain only one training point. The total number of unit cells area (1 km²) in the study area map is 56900 cells, while the surface occupied by the hydrocarbon fields represents 3120 cells, i.e. a little more than 5% of the total area. Thus, the areas occupied by oil and gas fields represent 2 and 3% respectively.

4.2 Application of the method

To the authors' best knowledge no study has investigated quantitatively the spatial association between known oil and gas accumulations and magnetic anomalies arising from shallow sedimentary section. In the most literature reviewed the characterization of this spatial correlation results from visual analysis (Burazer et al. 2001; Stone et al., 2004; Curto et al., 2012; Menshov et al., 2014).

In the application of the WofE method, hydrocarbon-related thematic map was overlapped with all 342 picked AS-SRM anomalies (Fig.3). The Weights of the Hydrocarbon-related theme in the model was calculated by using the relationship of the area covered by the oil and gas fields and the number of picked anomaly points that fall onto it. On the basis of this intersection, weights, contrasts and Studentized confidence values were calculated using equations (3, 4, 5, and 6).

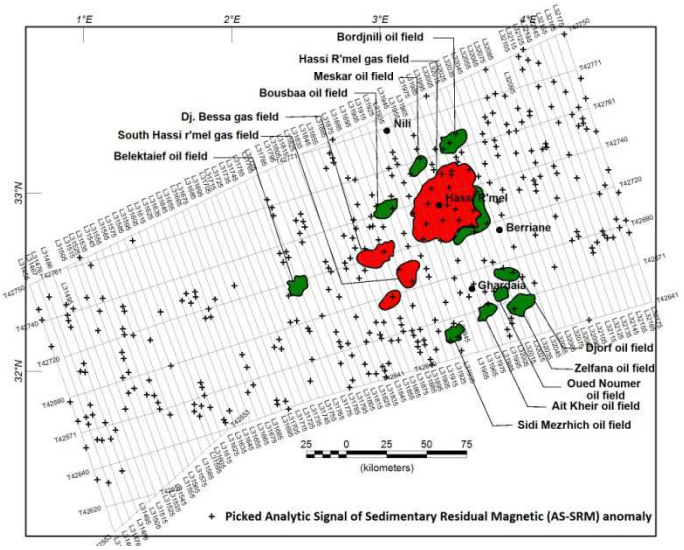

Figure 3. Location of picked AS-SRM anomalies

Initially all 342 picked anomalies are treated as being either present or absent in the model, and are not weighted by characteristics such as anomaly size or amplitude. The results show relatively low values of contrast 'C' (0.6 - 0.7) for oil and gas fields whether taken separately or together (Tab. 1). This indicates that the picked AS-SRM anomalies are practically *uncorrelated* with known hydrocarbon fields within the study area because of a somewhat random distribution of these anomalies as shown in figure 3.

Table 1. Summary of spatial association defined by weights of evidence model

Theme	W-	W+	C	St(c)
Oil	-0.01	0.58	0.59	2.0
Gas	-0.03	0.60	0.63	2.7
Oil+gas	-0.05	0.68	0.73	4.1

The magnitude of the analytic signal of picked anomalies ranges from 1.5 to 13.7 nT/km with an arithmetic mean of 2.8 nT/km and standard deviation of 1.8 nT/km. Their width ranges between 1.38 and 8.8 km with an average value of 3.27 km and standard deviation of 1.2 km. To give a quick visual summary of the picked anomalies, they were divided into ten class intervals (bins) according to their wavelengths and their magnitude values (Fig. 4). The number of ten bins is chosen according to Sturges' rule, which suggests that the number of intervals should be as close as possible to $1+log_2(N)$, where N is the number of anomalies. Magnitude of AS-SRM (Fig. 4a) shows a skewed distribution to the right with a large number of anomalies (nearly 65% of all anomalies) in the lower value class (leftmost side). An almost similar shape is obtained for the width of the anomalies (Fig. 4b), which exhibits some right-skew.

The problem with this distribution of anomaly classes is that some of the classes have a very small number occurring in them. This gives rise to a very noisy and unreliable weights, with poor estimates. The alternative is to calculate weights for classes whose intervals are selected so that each bin holds the same number of picked anomalies, and to examine the variation of the weights and contrast at each amplitude and wavelengths intervals.

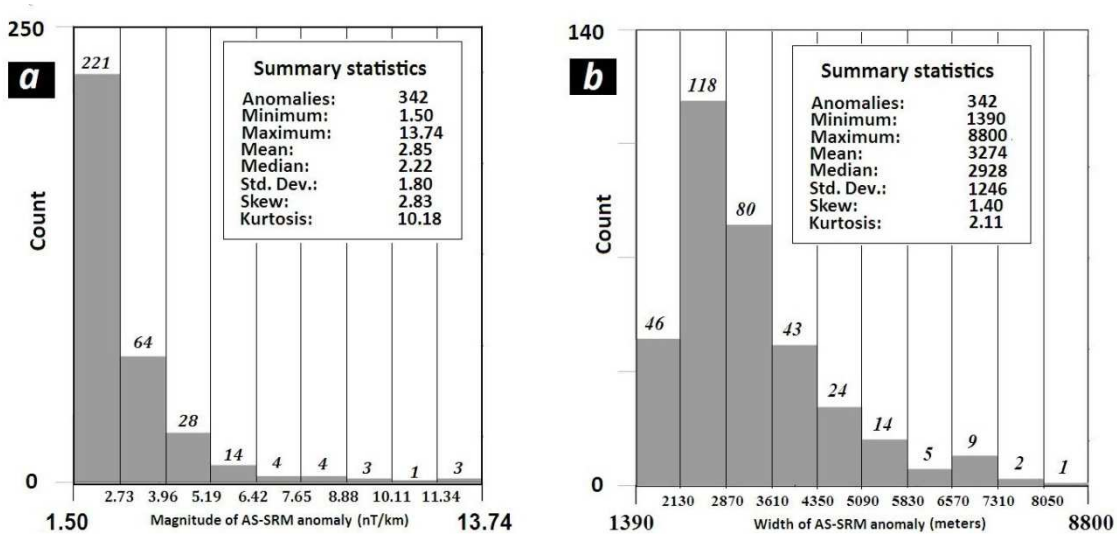

Figure 4. Frequency histogram of AS-SRM anomalies according to: (a) amplitude, (b) width.

5 RESULTS AND DISCUSSION

This study synthesizes results of the research work to develop and demonstrate the existence of relationship between oil and gas reservoirs distribution and Hydrocarbon Seepage-Induced Magnetic anomalies. Both gas and oil fields were alternately used as binary patterns in the weights of evidence (WofE) modeling for assessing their spatial association with AS-SRM anomalies, and to distinguish them from any other shallow-sourced magnetic signatures.

All picked anomalies were classified into 10 bins with varied width such that each bin contains 10% of the total of anomalies (i.e. about 34). The set of picked anomalies that fall into a defined class is used to calculate the weights for both oil and gas fields binary patterns, one weight per class, using the overlap relationships between the hydrocarbon fields and the various classes on the anomalies. Tables 2 and 3 report summary of weights, contrast and Studentized (*Confidence C_S)* for amplitude (nT/km) and size (km) for each class of AS-SRM anomalies respectively.

Table 2. Variation of weights for different amplitudes (nT/km) of AS-SRM anomalies with respect to hydrocarbon (gas and oil) fields

Class amp. (nT/km)	No. of anom.	W^+	W^-	Contrast (C)	Confidence
< 1.6	1	-0.630806	0.027001	-0.657808	-0.647955
1.6 – 1.7	0				
1.7 – 1.8	0				
1.8 – 2.0	0				
2.2 – 2.2	2	0.123321	-0.007705	0.131026	0.179358
2.2 – 2.6	1	-0.53838	0.024061	-0.562441	-0.553204
2.6 – 3.0	4	0.75645	-0.068365	0.824815	1.54863
3.0 – 3.5	**7**	**1.317028**	**-0.173782**	**1.490809**	**3.511591**
3.5 – 4.9	4	0.78632	-0.072415	0.858735	1.60906

Table 3. Variation of weights for different anomaly widths of analytic signal with respect to hydrocarbon fields.

Class width (km)	No. of points	W^+	W^-	Contrast (C)	Confidence
< 2 km	1	-0.659811	0.027868	-0.687679	-0.677672
2 – 2.3	2	0.092532	-0.005686	0.098218	0.134583
2.3 – 2.5	2	0.062661	-0.003789	0.06645	0.09114
2.5 – 2.7	1	-0.630806	0.027001	-0.657808	-0.647955
2.7 – 2.9	3	0.498318	-0.038494	0.536812	0.886106
2.9 – 3.3	1	-0.570146	0.025104	-0.59525	-0.585779
3.3 – 3.6	**7**	**1.346898**	**-0.18167**	**1.528568**	**3.586388**
3.6 – 4.1	4	0.727444	-0.064562	0.792006	1.489856
4.1 – 5.0	**8**	**1.480751**	**-0.22091**	**1.70166**	**4.184892**
>5 km	4	0.848876	-0.081355	0.930231	1.735263

It can be observed that the strongest spatial correlations are related to certain class of anomalies. They are defined by contrasts C > 1.5, and confidence C_S > 3.5 implying statistically significant for the classes of AS-SRM anomalies believed to result from near-surface sources induced by hydrocarbon microseepages have wavelengths in the intervals 3.3 - 3.6 km and 4.1 - 5.0 km and amplitudes ranging from 3.0 to 3.5 nT/km.

Plot of data over flight line No. 31905 located in the central part of the study area is presented in Figure 5. The analytic signal profile shows two anomalies with amplitude values of 2.9 and 3.5 nT/km and width of 4.9 and 3.8 km, which occur above Bousbaa oil field and South Hassi Rmel gas field respectively.

The identified near-surface anomalies in the Algerian Triassic basin suggest a possible relationship between certain type of sedimentary residual anomalies and hydrocarbon fields emplacement. This hypothesis has been supported by the statistical model which enabled the quantitatively characterization of the degree of spatial relationship.

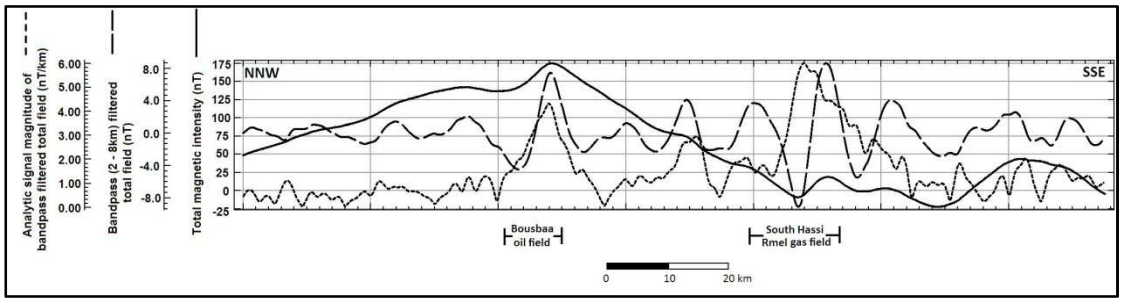

Figure 5. Aeromagnetic flight line profile L31905 across the Bousbaa oil field and the South Hassi Rmel gas field

6 CONCLUSION

Despite the availability of a large aeromagnetic coverage, these data were not always exploited in an optimal and rigorous way. In fact, they were only related, in the best of cases, to screen large areas for mapping depths to basement and bedrock structures. the results obtained from GIS-based weights of evidence analysis demonstrate that regional aeromagnetic data when acquired at relatively low altitude and at suitable accuracy can provide important information about intra-sedimentary features and residual anomalies attributed to long-term hydrocarbon microseepages. The application of spatial association analysis using GIS-based weights of evidence technique has successfully identified a particular class of sedimentary residual magnetic anomalies correlating directly with known underlying oil and gas accumulations within the Algerian Triassic basin. Even though this approach is empirical, it nonetheless provides support for determining successful and cost effective exploration strategies in predicting areas of high hydrocarbon potential where little or no exploration activity exists.

High resolution aeromagnetic surveys are certainly more suitable for this venture allowing to improve the definition of the observed aeromagnetic field so that small seep-induced effects can be better defined in order to detect more of them and to interpret them more accurately.

REFERENCES

Baouche R., Nedjari A., Eladj S. and Chaouchi R. 2009. Analysis and interpretation of environment sequence models in Hassi R'Mel Field in Algeria. *Energy problems and environmental engineering, p. 38-48.*

Bencherif, D., 2003. Giant Hassi R'Mel gas field. *AAPG Hedberg Conference, "Paleozoic and Triassic Petroleum Systems in North Africa", Algiers, Algeria.*

Berezkin V.M., Kiritchek M.A. and Kunarev A.A. 1978. Application of geophysical exploration methods for direct exploration of oil and gas, (*in russian*). *Nedra, 223 p.*

Burazer M., Grbović M., and Žitko V. 2001. Magnetic data processing for hydrocarbon exploration in the Pannonian Basin, Yugoslavia. *Geophysics, vol. 66, n°6, p. 1669-1679.*

Curto J.B., Pires A.C.B., Silva A.M., and Crósta A.P. 2012. The role of airborne geophysics for detecting hydrocarbon microseepages and related structural features: The case of Remanso do Fogo, Brazil. *Geophysics, vol. 77, no. 2, p. B35–B41.*

Donovan T.J., Forgey R. and Roberts A., 1979. Aeromagnetic detection of diagenetic magnetite over oil fields. *AAPG Bull., 63, 245−248.*

Flekkoy E.G. ; Legeydo, P. ; Haland, E. ; Drivenes, G. ; Kjerstad, J., 2013. Hydrocarbon detection through induced polarization: Case study from the Frigg area. *Annual International Meeting - Society of Exploration Geophysicists. 2, p.800-804, SEG Houston 2013.*

Foote R. S., 1996. Relationship of near-surface magnetic anomalies to oil- and gas-producing area, in D. Schumacher and M. A. Abrams, eds., Hydrocarbon migration and its near-surface expression: *AAPG Memoir 66, p. 111-126.*

Gay, Jr., S. P., 1992. Epigenetic versus syngenetic magnetite as a cause of magnetic anomalies: *Geophysics, v. 57, p. 60–68.*

Gay, Jr., S.P., and Hawley B.W., 1991. Syngenetic magnetic anomaly sources: three examples: *Geophysics, v. 56, p. 902–913.*

Klett, T.R., 2000. Total Petroleum Systems of the Trias/Ghadames Province, Algeria, Tunisia, and Libya -The Tanezzuft-Oued Mya, Tanezzuft-Melrhir, and Tanezzuft-Ghadames. *U.S. Geological Survey Bulletin 2202-C, http://greenwood.cr.usgs.gov/pub/bulletins/b2202-c/*

LeSchack, L. A., and Van Alstine, D.R. 2002. High-resolution ground-magnetic (HRGM) and radiometric surveys for hydrocarbon exploration: Six case histories in western Canada, *in Surface exploration case histories: Applications of geochemistry, magnetics, and remote sensing, D. Schumacher and L. A. LeSchack, eds., AAPG Studies in Geology 48, SEG Geophysical References Series 11, p. 67– 156.*

Machel, H.G., and Burton E.A., 1991. Causes and spatial distribution of anomalous magnetization in hydrocarbon seepage environments: *AAPG Bulletin, v. 75, p. 1864– 1876.*

Menshov O., Kuderavets R., Chobotok I., 2014. Magnetic investigations in Carpathian Foredeep of Ukraine. *Castle Meeting; New trends on Paleo, Rock and Environmental Magnetism; Evora, 2014.*

Perez-Perez A., D'Onofrio L., Bosch M., and Zapata E. 2011. Association between magnetic susceptibilities and hydrocarbon deposits in the Barinas-Apure Basin, Venezuela, *Geophysics. vol. 76, no. 6, p. L35–L41.*

Raines, G.L., 1999. Evaluation of weights of evidence to predict epithermal-gold deposits in the great basin of the Western United States. *Natural Resources Research 8, 257–276.*

Salati S. 2014. Characterization and remote detection of onshore hydrocarbon seep-induced alteration. *PhD dissertation thesis. Univesity of Twente, Faculty of Geo-Information science and Earth observation, ITS, Enschede, The Netherlands, 162 p.*

Saunders D.F., Burson K.R., Branch J.F., Thompson C.K., 1993. Relation of thorium normalized surface and aerial radiometric data to subsurface petroleum accumulations. *Geophysics, v. 58. p. 1417–1427.*

Saunders, D. F., K. R. Burson, and C. K. Thompson, 1991. Observed relation of soil magnetic susceptibility and soil gas hydrocarbon analysis to subsurface petroleum accumulations: *AAPG Bulletin, v. 75, p. 389–408.*

Schumacher D. and Foote R.S., 2014. Seepage-Induced Magnetic Anomalies Associated with Oil and Gas Fields: Onshore and Offshore Examples. *AAPG International Conference & Exhibition, Istanbul, Turkey, September 14-17, 2014.*

Schumacher D., 1996. Hydrocarbon-induced alteration of soils and sediments, *in* D. Schumacher and M. A. Abrams, eds., Hydrocarbon migration and its near-surface expression: *AAPG Memoir 66, p. 71–89.*

Schumacher D., 2000. Surface geochemical exploration for oil and gas: New life for an old technology. *The Leading Edge. p.258-261.*

Schumacher D., 2010. Integrating hydrocarbon microseepage data with seismic data doubles exploration success. *Proceedings, Indonesian petroleum association 34th annual conference and exhibition, may 2010*

Schumacher D., 2014. Minimizing Exploration Risk: The Impact of Hydrocarbon Detection Surveys for Distinguishing Traps with Hydrocarbons from Uncharged Traps. *GeoConvention 2014 CSEG CSPG CWLS Conference: FOCUS*

Spector A., and Grant F. S. 1970, Statistical Models for Interpreting Aeromagnetic Data, *Geophysics. 35, 293–302.*

Stone V.C.A., Fairhead D. J. and Oterdoom W.H., 2004. Micromagnetic seep detection in Sudan, *The Leading Edge; v. 23; n°. 8; p. 734-737.*